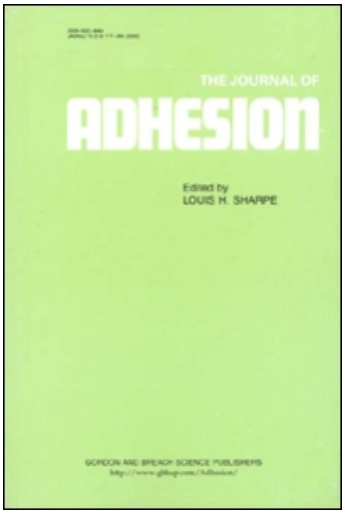

The Journal of Adhesion
Publication details, including instructions for authors and subscription information:
http://www.informaworld.com/smpp/title~content=t713453635

In Situ Imaging of Barnacle (*Balanus amphitrite*) Cyprid Cement Using Confocal Raman Microscopy

Martin Schmidt[a]; Andreia Cavaco[b]; Notburga Gierlinger[a]; Nick Aldred[b]; Peter Fratzl[a]; Michael Grunze[c]; Anthony S. Clare[b]
[a] Max Planck Institute of Colloids and Interfaces, Department of Biomaterials, Potsdam, Germany [b] School of Marine Science and Technology, Newcastle University, Newcastle Upon Tyne, United Kingdom [c] Applied Physical Chemistry, University of Heidelberg, Im Neuenheimer Feld, Heidelberg, Germany

To cite this Article Schmidt, Martin , Cavaco, Andreia , Gierlinger, Notburga , Aldred, Nick , Fratzl, Peter , Grunze, Michael and Clare, Anthony S.(2009) '*In Situ* Imaging of Barnacle (*Balanus amphitrite*) Cyprid Cement Using Confocal Raman Microscopy', The Journal of Adhesion, 85: 2, 139 — 151
To link to this Article: DOI: 10.1080/00218460902782279
URL: http://dx.doi.org/10.1080/00218460902782279

The Journal of Adhesion, 85:139–151, 2009

ISSN: 0021-8464 print/1545-5823 online
DOI: 10.1080/00218460902782279

Taylor & Francis
Taylor & Francis Group

In Situ Imaging of Barnacle (*Balanus amphitrite*) Cyprid Cement Using Confocal Raman Microscopy

Martin Schmidt[1], Andreia Cavaco[2], Notburga Gierlinger[1], Nick Aldred[2], Peter Fratzl[1], Michael Grunze[3], and Anthony S. Clare[2]

[1]Max Planck Institute of Colloids and Interfaces, Department of Biomaterials, Potsdam, Germany
[2]School of Marine Science and Technology, Newcastle University, Newcastle Upon Tyne, United Kingdom
[3]Applied Physical Chemistry, University of Heidelberg, Im Neuenheimer Feld, Heidelberg, Germany

Barnacles are a model for research on permanent underwater adhesion and the wider process of marine biofouling. A detailed understanding of the permanent adhesive secreted by the cypris larva for permanent settlement, the so-called cyprid cement, has potential to lead to novel antifouling solutions. There is a need for micro-analytical chemical in situ *methods to gain more insight into the process of adhesion and the chemical composition of the cement. In this study, the applicability of confocal Raman microscopy for imaging the cyprid cement beneath permanently attached juvenile barnacles (*Balanus amphitrite*) was explored. Based on acquired area scans Raman images for characteristic chemical functional groups were obtained. In addition to showing the morphology of the attachment apparatus, the images provided information on chemical composition, in particular the hydration state of the cement, and demonstrated the potential of this method for* in situ *studies of adhesion at the micro-scale.*

Keywords: Bioadhesion; Biofouling; Carotenoids; Microspectroscopy; Raman imaging

Received 1 October 2008; in final form 27 December 2008.

One of a Collection of papers honoring J. Herbert Waite, the recipient in February 2009 of *The Adhesion Society Award for Excellence in Adhesion Science, Sponsored by 3M*.

Address correspondence to Peter Fratzl, Max Planck Institute of Colloids and Interfaces, Department of Biomaterials, 14424 Potsdam, Germany. E-mail: peter.fratzl@mpikg.mpg.de

INTRODUCTION

Biological adhesion exhibits remarkable diversity, complexity, and range of performance, suggesting great potential for basic research and biomimetic applications [1–7]. Underwater adhesives are the key agents in the unwanted colonization of man-made structures by marine or freshwater organisms—a process known as biofouling, which is a considerable problem for maritime and aquaculture industries [8,9]. It is suggested that a more thorough understanding of the fundamental mechanisms of settlement and adhesion in fouling organisms may contribute to novel antifouling solutions. Particularly, the processes of bioadhesion at the molecular level are poorly understood and new insights are highly desirable.

Barnacles, the only sessile crustaceans, have the ability to firmly attach underwater to a wide variety of surfaces and constitute a model for research on permanent underwater adhesion [10]. At settlement, barnacles switch from a pelagic (larval) to benthic (adult) existence [11]. The transition involves three attachment processes [2,10]; the first being temporary attachment of the cypris larva (Fig. 1a), which allows exploration of foreign substrata through a poorly understood reversible mechanism [12–14]. Secondly, permanent settlement is initiated by the secretion of a proteinaceous "cyprid cement", deposited as a globular mass [15]. Subsequently, the cyprid undergoes metamorphosis to a juvenile barnacle (Fig. 1b) and grows to adulthood (Fig. 1c), remaining fixed to the surface *via* repetitive secretion of the adult cement [16]. A detailed understanding of the adult cement and its mode of action is emerging; however, the specific bonding interactions that occur in this extracellular multi-functional, multi-protein complex remain to be determined [2,10,17–19].

Colonising stages, such as the cyprid, are a target for antifouling approaches [14,20–22] and it is interesting, therefore, to note that the cyprid permanent cement, despite its significance, has received

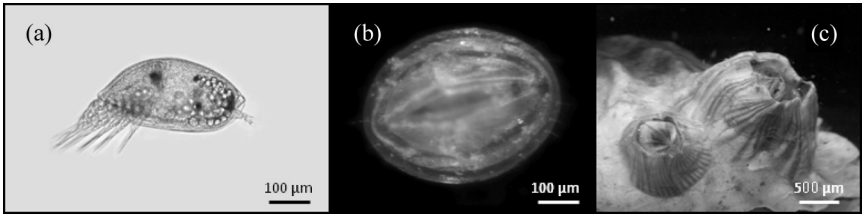

FIGURE 1 Three stages in the barnacle (*Balanus amphitrite*) life cycle: a) cypris larva, b) juvenile, and c) two adults.

far less attention than the adult cement in terms of past research [14]. One reason for this oversight may be that, for many years, the cyprid and adult cements were considered to be the same material [23]. At that time, cyprid temporary adhesion was also believed to occur through suction [23,24], and this now seems unlikely to be the case [14,25]. Molecular [26] and morphological [27] studies suggest that the adult cement and the cyprid permanent cement are unrelated. So far, the cyprid permanent cement has been investigated with regard to its composition *via* a histochemical approach [15] and its secretion [28,29]. Recently, atomic force microscopy was used to study the post-expression curing of cyprid permanent cement to further elucidate this complex system [30]. The cyprid cement is likely to be a heterogeneous material mainly composed of proteins [15]. The liquid components are released from cement glands in the body of the cyprid, through the antennular cement ducts. The liquid cement embeds the antennules externally, forming a globular disc ($<100\,\mu m$ diameter in *Balanus amphitrite*) [14]. The cement cures within a matter of hours [31], possibly *via* quinone-tanning [15].

In the study of biological adhesives in general, and the cyprid cement in particular, there is a recognized need for the application of *in situ* micro-analytical and chemical methods [1,10]. Amongst other techniques, micro-Raman and attenuated total reflection infrared spectroscopy have been used to study the chemistry of the adult calcareous basis and the process of reattachment in adult barnacles [32]. In fact, these *in situ* methods can provide chemical information without the need for cumbersome sample isolation. Scanning confocal micro-Raman spectroscopy was used in this preliminary study to observe the chemistry beneath the basis of recently metamorphosed juvenile barnacles (*Balanus amphitrite*), with particular attention being paid to the permanent cement plaque.

EXPERIMENT

Cypris larvae of *Balanus amphitrite* (from brood stock originally from Beaufort, North Carolina, USA) were reared according to [33]. Cyprids were transferred to glass fibre-filtered natural seawater ($0.2\,\mu m$, Whatman, Maidstone, UK), attracted to a cold light source and collected by pipette. The procedure was repeated three times to select only the healthiest cyprids and remove contaminants. Cyprids were stored at $6^{\circ}C$ and transported from Newcastle, UK to Potsdam, Germany, for experiments.

The substratum for settlement was an uncoated, acetone-washed glass microscopy cover slip ($24\,mm \times 40\,mm$, Carl Roth, Karlsruhe,

Germany). Juveniles were obtained by allowing approximately 20 cyprids to settle in 1 cm^3 beads of 3-isobutyl-1-methylxanthine (IBMX, 10^{-5} M, Sigma-Aldrich, Gillingham, UK, settlement inducer, for details see [34]) dissolved in artificial seawater (33 ppt, TropicMarin, Wartenberg, Germany). The cover slip was placed in a humid container and stored in the dark at room temperature for 16 hours. Permanent attachment to the glass cover slip and metamorphosis into juvenile barnacles was accomplished by a number of the allocated

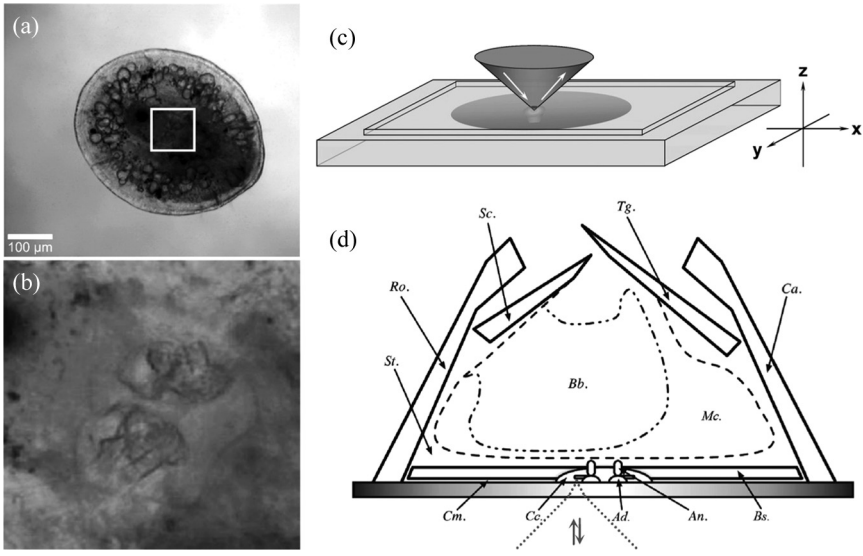

FIGURE 2 (a) Optical micrograph of a settled juvenile barnacle, with the white square marking the area containing the fully cured cement disc, which is shown in higher magnification in (b). The sampling geometry of the micro-Raman experiment is schematically shown in (c). (d) Schematic cross section of an adult barnacle on a glass substratum showing some of the shell plates – the rostrum (*Ro.*); carina (*Ca.*); scutum (*Sc.*), and tergum (*Tg.*). The cyprid antennules (*An.*) embedded in cyprid cement (*Cc.*) with the adhesive discs (*Ad.*) viewable from beneath the calcified basis (*Bs.*). The cyprid cement would be probed from beneath the interface between the glass and the barnacle. The adult cement [(*Cm*) not yet present in the juveniles studied] is secreted into the interface between the basis (*Bs.*) or base plate (calcified in a mature *B. amphitrite*, membraneous in a recently metamorphosed juvenile) and the glass substratum. The shell plates enclose the barnacle body (*Bb.*), or prosoma [suspended within a mantle cavity (*Mc.*)], and other soft tissues (*St.*), e.g., muscle and ovarian tissue. Note that the juvenile barnacles used in this study had yet to calcify their shell plates and basis.

larvae. The cover slip with the attached juvenile barnacles was inverted and transferred to the concavity of a glass microscope cavity slide, with the depression being filled by artificial seawater. The edges of the cover slip were sealed onto the glass slide to prevent evaporation of water. This measurement chamber was placed in a confocal Raman microscope (alpha300 R, WITec, Ulm, Germany) and a live juvenile barnacle was selected for measurement after locating and surveying the samples using the moveable x-y-z-stage. The cyprid cement beneath the juvenile basis was evident in the optical micrographs recorded in the microscope allowing its area to be mapped and imaged by scanning micro-Raman spectroscopy (see Figs. 2a and b).

The sampling geometry of the Raman experiment is schematically shown in Figs. 2c and d. Spectra were acquired with the confocal Raman microscope which is equipped with a piezoelectric scan stage at a $60\times$ microscope objective (Nikon, Düsseldorf, Germany, NA = 0.8). In order to gain high spatial resolution, a laser in the visible wavelength range (frequency-doubled Nd:YAG laser, $\lambda = 532\,\text{nm}$) was focused with a nearly diffraction-limited spot size ($\sim 0.61\lambda/\text{NA} \approx 400\,\text{nm}$) onto the sample and the Raman light was detected by a CCD camera (DV401-BV, Andor, Belfast, UK) behind a spectrometer (UHTS 300, WITecUlm, Germany) with a spectral resolution of $3\,\text{cm}^{-1}$. The laser power on the sample was approximately 5 mW. The sample was mapped in 1 μm steps recording spectra with an integration time of 0.3 s per pixel or scan. The WITec Project software (version 1.90) was used for spectral and image processing. Chemical images were computed from the two-dimensional spectral map using a sum filter, which integrates the intensity over a defined wavenumber range in the Raman spectra, using a background subtraction by applying a baseline from the first to the second spectral border. This experiment was performed repeatedly, with cyprids aged for between 6–9 days prior to settlement, to ensure reproducibility of the results.

RESULTS AND DISCUSSION

Figure 3a shows a typical as well as a very intense Raman spectrum recorded within an embedded antennule in the cyprid cement. The observed high intensity Raman bands are attributed to carotenoids (see Table 1) that cause resonance enhancement. Figure 3b shows three Raman spectra recorded from the cement plaque in areas surrounding the antennules. It is noted that the spectral bands in this case are much weaker. In order to improve the signal-to-noise ratio, average spectra were computed and the average spectrum from 50 individual spectra is presented (Fig. 3b). There are no bands found

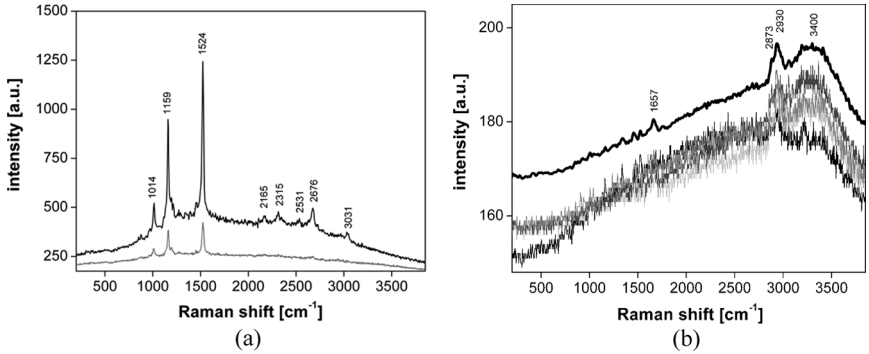

FIGURE 3 (a) A typical (gray) and a very intense Raman spectrum (black) recorded within an antennule in the cyprid cement. (b) Three Raman spectra (shades of gray) recorded in the cement disc in areas surrounding the antennules, the average spectrum from 50 individual spectra (offset, bold black), and, for comparison, a Raman spectrum recorded near to the cyprid cement (thin black).

from carotenoids. Instead, the amide I band of proteins around 1657 cm^{-1}, C–H stretching bands at 2873 and 2930 cm^{-1}, and the broad O–H stretching band around 3400 cm^{-1} are observed (*cf.* Table 1). A typical Raman spectrum recorded in close proximity to the cyprid cement is also shown in Fig. 3b.

Figure 4a shows an optical micrograph of the cyprid cement of a permanently attached juvenile barnacle, imaged from beneath the

TABLE 1 Band Assignments of Spectra Measured in the Cyprid Cement Disc in Juvenile Barnacle *Balanus amphitrite*

Band position [cm^{-1}]	Assignment
Carotenoids in the antennules (Refs. [41] and [42])	
1014	ν_3 (C–CH_2 stretching)
1159	ν_2 (C–C stretching)
1524	ν_1 (conjugated C=C stretching)
2165	$\nu_2+\nu_3$
2315	$2\nu_2$
2531	$\nu_1+\nu_3$
2676	$\nu_1+\nu_2$
3031	$2\nu_1$
Components in the cement disc	
1657	amide I of proteins
2873	CH_3 symmetric stretching
2930	CH_2 antisymmetric stretching
~3400	O–H stretching of water

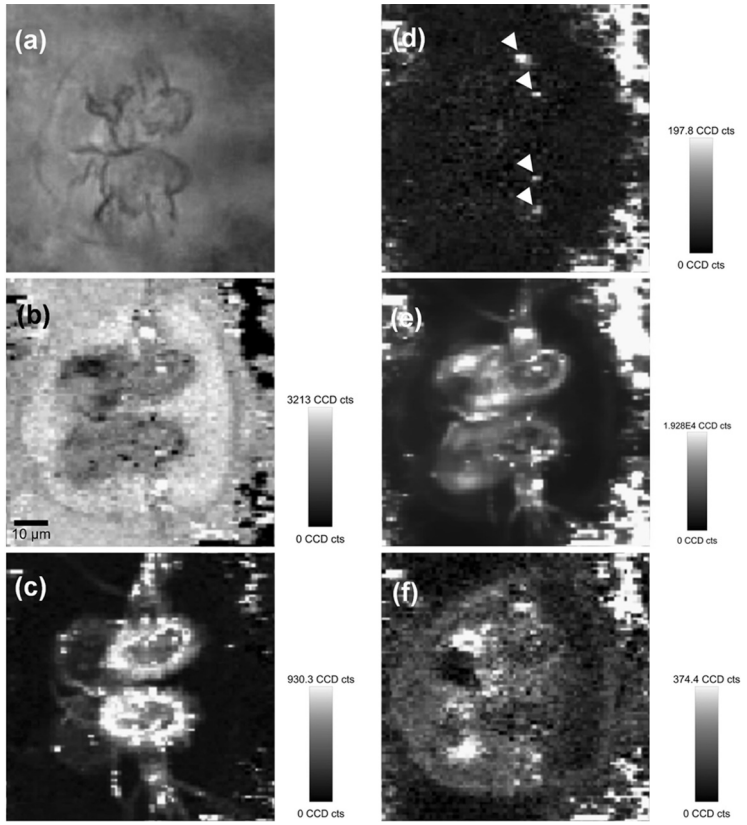

FIGURE 4 (a) Optical micrograph of the cement disc of a permanently attached juvenile barnacle mapped *in situ* by confocal micro-Raman spectroscopy. (b) Chemical Raman image derived by integrating the intensity of the O–H stretching vibration (3000–3800 cm^{-1}). Images for (c) the conjugated C=C stretching vibration of carotenoids (1480–1580 cm^{-1}), (d) the amide I band of proteins (1620–1680 cm^{-1}; the white arrows highlight four small areas of intense fluorescence), (e) the fluorescence background (2200–2500 cm^{-1}), and (f) the C–H stretching bands (2800–3000 cm^{-1}).

interface between the glass and the barnacle. The sample was mapped *in situ* by confocal micro-Raman spectroscopy. Several chemical images were derived from the position-resolved spectroscopic measurements, where differences in contrast were based on the recorded intensities in the different selected spectral regions (see Figures 4b–f and *cf.* Figures 3a and b). These images clearly illustrate the morphology and boundaries of both the cyprid cement (Figs. 4b and f)

and the embedded pair of antennules (Figs. 4b, c, and e), and show good agreement with optical micrographs (*cf.* Fig. 4a).

Figure 4b was obtained by integrating over the wavenumber range from 3000 to 3800 cm^{-1}, which is sensitive to O–H stretching vibrations (see Table 1) and indicative of the spatial distribution of water. Despite considerable fluorescence and the fact that water is a weak Raman scatterer, the results were suggestive of increased quantities of water in the cured permanent cement relative to the surrounding area (*cf.* Fig 3b). Adhesive secreted by zoospores of the fouling alga *Ulva* is known to swell, on secretion, to approximately ten times its original size through incorporation of water [35,36]. In the case of cyprid cement, it has been speculated that constitutive water molecules would be essential for stabilization of the molecular conformation of cement proteins [10,15]. Fig. 4b is, therefore, supportive of the theory that water might play an important role in cement curing and function. An alternate explanation is an abundance of polar (–OH) groups in the cured cement, as has been noted for mussel byssal adhesive [37]. In mussel byssus, these polar groups (contributed by large mole % concentrations of DOPA in the byssus peptides) are believed to enhance adhesion [38,39] and assist in the wetting of immersed high-energy materials [40].

The image in Fig. 4c was computed by integrating over the band originating from the conjugated C=C stretching vibration of carotenoids [41,42] at 1524 cm^{-1} (integrating from 1480 to 1580 cm^{-1}). The paired antennules within the boundaries of the cement are discernible. Interestingly, the distribution of carotenoids is restricted to the outer margin of the antennular discs and extends laterally from these structures (Fig. 4c), indicating that the intense carotenoid signal is localized to the contact points between the cyprid cuticle and the surface. The cuticular villi of the disc and the velum that surrounds the margins of the disc [43,44] could account for this strong signal. It has been hypothesized that the cuticular villi make contact with the surface that is being explored [25,45] and the results presented here are consistent with this hypothesis. It is also possible that the carotenoid signal could arise from the cyprid's antennular secretion that is deposited as "footprints" during exploration of some surfaces. Cyprid footprints have the characteristic "halo" shape that is apparent in Fig. 4c (*cf.* Ref. [46] (Fig. 5)), although in this figure the halo is larger than previously reported (*cf.* Refs. [27] (Fig. 4), [45] (Fig.2)). It seems unlikely, however, that such high concentrations of carotenoids would be found in the footprint, although this can be investigated in future studies by (surface-enhanced) Raman spectroscopy of surfaces that have previously been explored by cyprids. Further, if the signal in

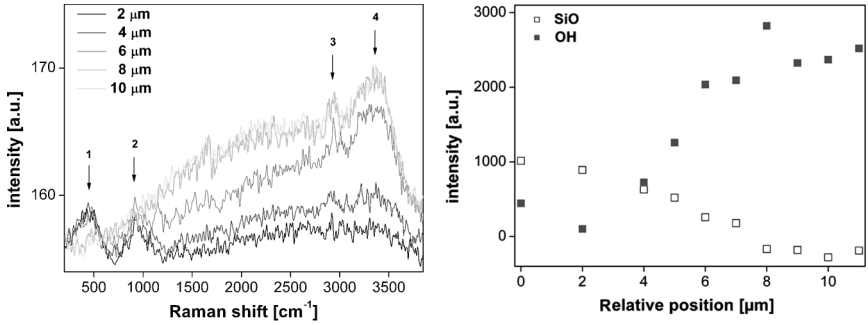

FIGURE 5 (a) Z-position-dependent Raman spectra (each an average of 9 individual spectra) across the glass-cement interface. As the Raman bands (1) just below 500 cm^{-1} and (2) around 930 cm^{-1}, both attributable to glass, vanish, the (3) C–H and (4) O–H stretching bands of the cement disc emerge. (b) Plots of the z-position-dependent intensities for the SiO band below 500 cm^{-1} (integrated between 200 and 700 cm^{-1}) and the O–H stretching vibration (3000–3800 cm^{-1}).

Fig. 4c were from the footprint material, then it would be expected to provide a protein signal in the amide I band (Fig. 4d). Finally, any footprint material on the attachment disc's surface would, presumably, be masked or removed by the subsequent secretion of the permanent cement.

Carotenoids have been reported in barnacles [47,48] and are common among other Crustacea [49]. As such, their suggested role is as antioxidants [49] and as membrane reinforcers, for example in cuticle [50]. Further study will be required to confirm the identity of the putative carotenoids and their function.

The intensity distribution of the amide I band of proteins at 1657 cm^{-1} (1620–1680 cm^{-1}, containing also spectral contributions from the bending mode of water) is shown in Fig. 4d with the fluorescence background (2200–2500 cm^{-1}) as a control in Fig. 4e. The intensity distribution of the C–H stretching bands (2800–3000 cm^{-1}) is presented in Fig. 4f. The spatial distribution of the signal from the C–H stretching bands is strong evidence that the cyprid cement has an organic matrix. Despite the fact that the cyprid cement is known to contain proteinaceous components [15,30,51], the amide I band signal is low. This may be due to the limited sensitivity in the measurement and the short integration time (0.3 s) per measurement spot. The short integration time was chosen in order to avoid sample damage from the laser irradiation and to allow acquisition of the

mapping data in a reasonable time (~45 min). It is noted that the amide N–H stretching was not discernible and it may be obscured by the broad O–H stretching band.

Across all the chemical images (Figs. 4b–f), four small areas of high signal intensity are observed, seen most clearly in Fig. 4d (see white arrows). These spots are due to strong fluorescence and may mark points of contact between antennular setae and the substratum. The most likely candidates for the spot within the boundary of each disc are postaxial seta 3 and/or the axial seta [44,52]; the other two spots may be points of contact between the four subterminal setae of each antennule and the substratum [44,53,54].

In contrast to optical micrographs, imaging with confocal micro-Raman spectroscopy not only visualizes the morphology of the cement disc but also provides specific information on the chemical composition. This chemical analysis is performed non-destructively, *in situ*, and without the need for difficult sample isolation. Due to the confocal measurement geometry, the technique is sensitive to the interface [55], as was confirmed by z-scans probing the depth resolution. Figure 5 gives the result of a micrometric z-scan across the glass-cement interface of the sample shown in Fig. 4. Figure 5a shows five z-position-dependent Raman spectra. As the focal spot was stepped across the interface into the sample, the Raman bands just below 500 cm^{-1} and around 930 cm^{-1}, which are both attributable to glass [56], vanished, and the C–H and O–H stretching bands of the cement emerged (see Fig. 5b). This illustrates the critical capability of the technique to directly probe the cement disc at the substratum interface.

Attenuated total reflection infrared spectroscopy, a complementary vibrational spectroscopic technique, is also surface-sensitive and its applicability for live cell adhesion assays was recently demonstrated [57]. It was suggested earlier that it would also be suitable for investigations of marine biofouling [58] and it was most recently implemented in the *in situ* spectroscopic investigation of *Perna canaliculus* mussel larvae primary settlement [59]. In the present study of barnacles, however, the spatial resolution, scanning capabilities, and correlation with optical micrographs provided by the micro-Raman approach were advantageous and desirable [60]. Importantly, in addition to imaging individual specimens, it enabled selection of the area of interest (*cf*. Fig. 2a) and, thus, spatial as well as spectral discrimination from the background.

The authors envisage application of this technique to dynamic chemical imaging *during* the settlement of the cypris larvae to the substratum. However, the current measurement time is insufficient,

which may be improved, *e.g.*, by imaging a smaller area or by lowering the spatial resolution and by using a spectroscopic electron multiplying CCD camera as a detector [61]. It is also noted that there will be a trade-off between the desired chemical sensitivity in the measurement and the required acquisition time. Radiation-induced sample damage must also be avoided when the same area is measured continually. Finally, it is known that there are substrate-specific phenotypic differences in the morphology and chemistry of adult barnacle adhesive deposited onto different surface types [2,62,63] and, with this in mind, observing the effects of substratum on cyprid cement would be an interesting avenue of investigation.

CONCLUSIONS

The cyprid cement beneath individual permanently attached juvenile barnacles (*B. amphitrite*) was imaged by scanning confocal Raman microscopy without sample invasion or isolation. Along with visualizing the morphology of the cement disc, information on the chemical composition, including the hydration state, was gained. The considerable concentration of –OH groups detected in the cement provides evidence that water may play a role in the cement curing process. Carotenoids, which are components of crustacean cuticle, were identified at the periphery of the antennular attachment disc suggesting that this region of the disc makes contact with the substratum and perhaps contributes to adhesion.

The sensitivity to the interface between the adhesive and the substratum, the spatial resolution, and the scanning capabilities are key features of the approach. This preliminary study demonstrated the potential of the method, and its application to dynamic, chemical, *in situ* imaging during the settlement of cypris larvae on different substrata is a future aspiration.

ACKNOWLEDGMENTS

The authors acknowledge financial support by the Max Planck Society and the EC Framework 6 Integrated Project “AMBIO”. The views expressed in this publication reflect only those of the authors and the Commission is not liable for any use that may be made of the information contained therein. A special thanks to Sheelagh Conlan (Newcastle) for the cyprid culture. Notburga Gierlinger acknowledges financial support by the APART programme of the Austrian Academy of Sciences.

REFERENCES

[1] Smith, A. M. and Callow, J. A., *Biological Adhesives*, (Springer, Berlin, 2006).
[2] Wiegemann, M., in *Adhesion – Current Research and Application*, W. Possart (Ed.) (Wiley-VCH, Weinheim, 2005), Ch. 10, pp. 143–156.
[3] Lin, Q., Gourdon, D., Sun, C., Holten-Andersen, N., Anderson, T. H., Waite, J. H., and Israelachvili, J. N., *PNAS* **104**, 3782–3786 (2007).
[4] Waite, J. H., Andersen, N. H., Jewhurst, S., and Sun, C. J., *J. Adhes.* **81**, 297–317 (2005).
[5] Smith, B. L., Schaffer, T. E., Viani, M., Thompson, J. B., Frederick, N. A., Kindt, J., Belcher, A., Stucky, G. D., Morse, D. E., and Hansma, P. K., *Nature* **399**, 761–763 (1999).
[6] Lee, H., Lee, B. P., and Messersmith, P. B., *Nature* **448**, 338–341 (2007).
[7] Fratzl, P. and Weinkamer, R., *Prog. Mater. Sci.* **52**, 1263–1334 (2007).
[8] Yebra, D. M., Kiil, S., and Dam-Johansen, K., *Prog. Org. Coat.* **50**, 75–104 (2004).
[9] Schultz, M. P., *Biofouling* **23**, 331–341 (2007).
[10] Kamino, K., in *Biological Adhesives*, A. M. Smith and J. A. Callow (Eds.) (Springer, Berlin, 2006), Ch. 8, pp. 145–165.
[11] Anderson, D. T., *Barnacles: Structure, Function, Development and Evolution*, (Chapman and Hall, London, 1994). Ch. 1, pp. 1–25.
[12] Walker, G. and Yule, A. B., *J. Mar. Biol. Ass. U.K.* **64**, 679–686 (1984).
[13] Dreanno, C., Kirby, R. R., and Clare, A. S., *Biol. Lett.* **2**, 423–425 (2006).
[14] Aldred, N. and Clare, A. S., *Biofouling* **24**, 351–363 (2008).
[15] Walker, G., *Mar. Biol.* **9**, 205–212 (1971).
[16] Yule, A. B. and Walker, G., in *Crustacean Issues 5: Barnacle Biology*, A. J. Southward (Ed.) (A. A. Balkema, Rotterdam, 1987), pp. 389–402.
[17] Kamino, K., Inoue, K., Maruyama, T., Takamatsu, N., Harayama, S., and Shizuri, Y., *J. Biol. Chem.* **275**, 27360–27365 (2000).
[18] Kamino, K., *Biochem. J.* **356**, 503–507 (2001).
[19] Wiegemann, M., Kowalik, T., and Hartwig, A., *Mar. Biol.* **149**, 241–246 (2006).
[20] Visscher, J. P., *Biol. Bull.* **54**, 327–335 (1928).
[21] Houghton, D. R., *Underwater Sci. Technol. J.* **2**, 100–105 (1970).
[22] Clare, A. S. and Aldred, N., in *Advances in Marine Antifouling Coatings and Technologies*, C. Hellio and D. Yebra (Eds.) (Woodhead Publishing Ltd., in press).
[23] Lindner, E. and Dooley, C. A., Unpublished report from the San Francisco Bay Naval Shipyard, Vallejo, California, Paint laboratory. Report No. 69–3, AD856070 (1969).
[24] Saroyan, J. R., Lindner, E., and Dooley, C. A., *Biol. Bull.* **139**, 333–350 (1970).
[25] Phang, I. Y., Aldred, N., Ling, X. Y., Tomczak, N., Huskens, J., Clare, A. S., and Vancso, G. J., *J. Adhes.* in press.
[26] Kamino, K. and Shizuri, Y., in *New Developments in Marine Biotechnology*, Y. Le Gal and H. O. Halvorson (Eds.) (Plenum Press, New York, 1998), pp. 77–80.
[27] Aldred, N., Phang, I. Y., Conlan, S. L., Clare, A. S., and Vancso, G. J., *Biofouling* **24**, 97–107 (2008).
[28] Okano, K., Shimizu, K., Satuito, C. G., and Fusetani, N., *J. Exp. Biol.* **199**, 2131–2137 (1996).
[29] Ödling, K., Albertsson, C., Russell, J. T., and Mårtensson, L. G. E., *J. Exp. Biol.* **209**, 956–964 (2006).
[30] Phang, I. Y., Aldred, N., Clare, A. S., Callow, J. A., and Vancso, G. J., *Biofouling* **22**, 245–250 (2006).
[31] Pettitt, M. E., Henry, S. L., Callow, M. E., Callow, J. A., and Clare, A. S., *Biofouling* **20**, 299–311 (2004).

[32] Dickinson, G. H., Ramsay, D., Russell, Jr., J. N., Rittschof, D., and Wahl, K. J., unpublished, presented at the AVS 54th International Symposium, Seattle, WA, USA (2007).
[33] Hellio, C., Marechal, J.-P., Véron, B., Bremer, G., Clare, A. S., and Le Gal, Y., *Marine Biotechnology* **6**, 67–82 (2004).
[34] Clare, A. S., Thomas, R. F., and Rittschof, D., *J. Exp. Biol.* **198**, 655–664 (1995).
[35] Callow, J. A., Crawford, S. A., Higgins, M. J., Mulvaney, P., and Wetherbee, R., *Planta* **221**, 641–647 (2000).
[36] Callow, J. A., Osborne, M. P., Callow, M. E., Baker, F., and Donald, A. M., *Colloids Surf. B-Biointerfaces* **27**, 315–321 (2003).
[37] Wiegemann, M., *Aquat. Sci.* **67**, 166–176 (2005).
[38] Yu, M. E., Hwang, J. Y., and Deming, T. J., *J. Am. Chem. Soc.* **121**, 5825–5826 (1999).
[39] Lee, H., Scherer, N. F., and Messersmith, P. B., *PNAS* **103**, 12999–13003 (2006).
[40] Aldred, N., Ista, L. K., Callow, M. E., Callow, J. A., Lopez, G. P., and Clare, A. S., *J. R. Soc. Interface* **3**, 37–43 (2006).
[41] Howard, Jr., W. F., Nelson, W. H., and Sperry, J. F., *Appl. Spectrosc.* **34**, 72–75 (1980).
[42] Pézolet, M., Pigeon-Gosselin, M., Nadeau, J., and Caillé, J.-P., *Biophys. J.* **31**, 1–8 (1980).
[43] Nott, J. A., *Mar. Biol.* **2**, 248–251 (1969).
[44] Glenner, H. and Høeg, J. T., *J. Crustacean Biol.* **15**, 523–536 (1995).
[45] Phang, I. Y., Aldred, N., Clare, A. S., and Vancso, G. J., *J. R. Soc. Interface* **5**, 397–401 (2008).
[46] Walker, G., Cirripedia, in *Microscopic Anatomy of Invertebrates*, F. W. Harrison and A. G. Humes (Eds.) (Wiley-Liss, New York, 1992). Vol. 9 Crustacea, Ch. 5, pp. 249–311.
[47] Herring, P. J., *Cell. Mol. Life Sci.* **27**, 1027–1028 (1971).
[48] Matsuno, T., *Fish. Sci.* **67**, 771–783 (2001).
[49] Ghidalia, W. in *The Biology of Crustacea: Integument, Pigments and Hormonal Processes*, D. E. Bliss and L. H. Mantel (Eds.) (Academic Press, London, 1985), pp. 301–394.
[50] Vershinin, A., *BioFactors* **10**, 99–104 (1999).
[51] Walker, G., *J. Adhes.* **12**, 51–58 (1981).
[52] Nott, J. A. and Foster, B. A, *Phil. Trans. R. Soc. Lond. B* **256**, 115–134 (1969).
[53] Gibson, P. H. and Nott, J. A., *Fourth European Marine Biology Symposium*, (Cambridge University Press, Cambridge, 1971). pp. 227–236.
[54] Clare, A. S. and Nott, J. A., *J. Mar. Biol. Assoc. U. K.* **74**, 967–970 (1994).
[55] Everall, N., *Appl. Spectrosc.* **62**, 591–598 (2008).
[56] Etchepare, J., *Spectrochim. Acta* **26A**, 2147–2154 (1970).
[57] Schmidt, M., Wolfram, T., Rumpler, M., Tripp, C. P., and Grunze, M., *Biointerphases* **2**, 1–5 (2007).
[58] Hutson, T. B., Mitchell, M. L., Keller, J. T., Long, D. J., and Chang, M. J. W., *Anal. Biochem.* **174**, 415–422 (1988).
[59] Petrone, L., Ragg, N. L. C., and McQuillan, A. J., *Biofouling* **24**, 405–413 (2008).
[60] Salzer, R., Steiner, G., Mantsch, H. H., Mansfield, J., and Lewis, E. N., *Fresenius J. Anal. Chem.* **366**, 712–726 (2000).
[61] Dieing, T. and Hollricher, O., *Vib. Spectrosc.* **48**, 22–27 (2008).
[62] Berglin, M. and Gatenholm, P., *Colloids Surf. B-Biointerfaces* **28**, 107–117 (2003).
[63] Mori, Y., Urushida, Y., Nakano, M., Uchiyama, S., and Kamino, K., *FEBS J.* **274**, 6436–6446 (2007).